Article

Current Biology

Selective Activation of a Putative Reinforcement Signal Conditions Cued Interval Timing in Primary Visual Cortex

Highlights

- Reward-timing activity can be behaviorally conditioned in mouse V1
- Activating BF or cholinergic innervation conditions cued interval timing
- Cued interval timing in V1 is bidirectionally modifiable and is scale invariant
- V1 is a substrate for reinforcement learning and expression of temporal intervals

Authors

Cheng-Hang Liu, Jason E. Coleman, Heydar Davoudi, Kechen Zhang, Marshall G. Hussain Shuler

Correspondence

shuler@jhmi.edu

In Brief

Reward-timing activity arises in V1 when pairing visual cues with delayed reward, epitomizing how the brain predicts the timing of behaviorally relevant events. Liu et al. show that activation of basal forebrain or cholinergic input in V1 is sufficient to encode such activity, thereby advancing a mechanistic understanding of reinforcement learning.

Liu et al., 2015, Current Biology *25*, 1551–1561
June 15, 2015
http://dx.doi.org/10.1016/j.cub.2015.04.028

CellPress

Current Biology
Article

Selective Activation of a Putative Reinforcement Signal Conditions Cued Interval Timing in Primary Visual Cortex

Cheng-Hang Liu,[1] Jason E. Coleman,[2,3] Heydar Davoudi,[4] Kechen Zhang,[4] and Marshall G. Hussain Shuler[1,*]
[1]Solomon H. Snyder Department of Neuroscience, The Johns Hopkins University School of Medicine, Baltimore, MD 21205, USA
[2]The Picower Institute for Learning and Memory, Howard Hughes Medical Institute, Massachusetts Institute of Technology, Cambridge, MA 02139, USA
[3]Child Health Research Institute, Department of Pediatrics, University of Florida College of Medicine, Gainesville, FL 32610, USA
[4]Department of Biomedical Engineering, Johns Hopkins University School of Medicine, Baltimore, MD 21205, USA
*Correspondence: shuler@jhmi.edu
http://dx.doi.org/10.1016/j.cub.2015.04.028

SUMMARY

As a consequence of conditioning visual cues with delayed reward, cue-evoked neural activity that predicts the time of expected future reward emerges in the primary visual cortex (V1). We hypothesized that this reward-timing activity is engendered by a reinforcement signal conveying reward acquisition to V1. In lieu of behavioral conditioning, we assessed in vivo whether selective activation of either basal forebrain (BF) or cholinergic innervation is sufficient to condition cued interval-timing activity. Substituting for actual reward, optogenetic activation of BF or cholinergic input within V1 at fixed delays following visual stimulation entrains neural responses that mimic behaviorally conditioned reward-timing activity. Optogenetically conditioned neural responses express cue-evoked temporal intervals that correspond to the conditioning intervals, are bidirectionally modifiable, display experience-dependent refinement, and exhibit a scale invariance to the encoded delay. Our results demonstrate that the activation of BF or cholinergic input within V1 is sufficient to encode cued interval-timing activity and indicate that V1 itself is a substrate for associative learning that may inform the timing of visually cued behaviors.

INTRODUCTION

A fundamental task accomplished by the brain is the ability to predict the timing of behaviorally salient events. When environmental cues reliably precede future outcomes, neural mechanisms that learn the relationships and produce the interceding intervals offer a potential advantage by informing timed actions necessary to achieve expected outcomes. While numerous brain regions exhibit activity correlated with expected events [1–4], the neural mechanisms responsible for engendering temporal intervals elicited by behaviorally relevant cues remain largely unknown [5]. Exemplifying this issue and motivating the work presented here is the finding that pairing visual stimuli with delayed reward leads to the emergence of stimulus-evoked activity in the primary visual cortex (V1) that predicts the timing of expected future reward [6, 7].

The observation of reward-timing activity in V1—the earliest stage of cortical processing of visual information—may be regarded as a reflection of event-anticipatory activity first established elsewhere in the brain. An unconventional yet plausible alternative is that this activity is present due to learning-induced changes local to V1. A computational model inspired by the report of reward timing in V1 provides a general solution as to how V1 could, in principle, learn and express arbitrary cue-reward intervals de novo [8]. This model describes the emergence of reward-timing activity as resulting from a process of reinforcement learning [9], wherein a signal conveying behavioral outcome permits the modification of recently active synapses to encode the cue-reward delay. A critical component of this model, therefore, is the provision of this reinforcement signal. Should our model be applicable to the emergence of reward timing within V1, V1 itself must be a substrate of learning-induced changes controlled by such a signal.

A potential source providing this reward-related information is the basal forebrain (BF) as it projects directly and abundantly to V1 [10–14] and is responsive to the acquisition of reward [15–17]. Electrical stimulation of BF has been shown to enhance food and water intake [18], as well as self-administration behaviors [19]. In addition, pathological damage or experimental lesion of BF can cause substantive deficits in learning and memory [12, 20, 21]. Further, BF inputs in the neocortex are known to mediate cortical synaptic plasticity and have been implicated in various cognitive functions [6, 12, 15, 22–28]. Together, these observations give good cause to investigate whether BF inputs are sufficient to encode visually cued reward-timing activity.

We therefore tested the hypothesis that conditioning visually evoked responses in vivo by optogenetically driving BF input within V1 at fixed temporal delays—mimicking the presumed effects of actual reward acquired behaviorally—results in reward-timing-like activity. We demonstrate in mouse V1 that cue-evoked "reward"-timing activity is indeed elicited by selective activation of BF input, as its defining features are recapitulated

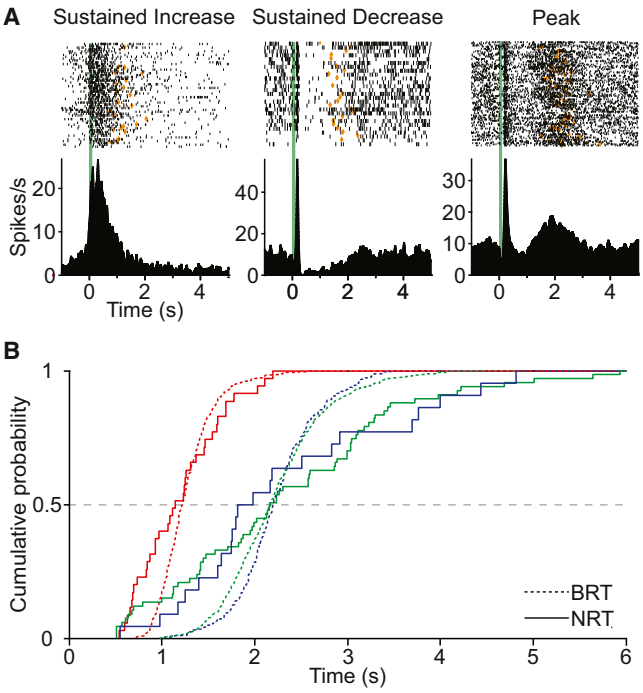

Figure 1. Reward-Timing Activity in Mouse V1

(A) Stimulus-evoked responses recorded from behaviorally conditioned animals exemplifying each of three reward-timing response forms: sustained increase, sustained decrease, and peak. Spike activity is aligned to the onset of transient (100 ms) full-retinal illumination (green bars), presented through head-mounted goggles (as illustrated in Figure 2A) for all unrewarded trials of a recording session. Orange symbols in the raster plots indicate the time the required number of licks to acquire reward was accomplished in each trial.

(B) Cumulative distribution functions of behavioral (dashed) and neural (solid) data. Recordings from three mice: mouse #1 (red), #2 (green), and #3 (blue). Required number of licks to reward: seven for mouse #1; ten for mouse #2 and #3. BRT (behaviorally experienced reward times, dashed lines): intervals between cue (green bars in A) and expected reward times (orange symbols in A) from multiple training sessions ($p < 10^{-7}$ for mouse #1 versus #2; $p < 10^{-7}$ for mouse #1 versus #3; $p = 0.21$ for mouse #2 versus #3; Wilcoxon rank-sum test). NRT (neural reports of time, solid lines): neural reports of intervals extracted from post-stimulus spike modulation as described in Experimental Procedures ($n = 35$ for mouse #1, 74 for #2, and 22 for #3; $p = 2 \times 10^{-5}$ for #1 versus #2; $p = 3 \times 10^{-5}$ for #1 versus #3; $p = 0.8$ for mouse #2 versus #3; Wilcoxon rank-sum test).

by this manipulation. Our data also demonstrate that optogenetically entrained timing activity in V1 can be bidirectionally tuned to represent new conditioning intervals, is subject to experience-dependent refinement, and may serve as a neural correlate of the commonly reported "temporal scalar property" [29, 30]. We further examined the neuromodulatory nature of the putative reinforcement signal responsible for engendering cued interval-timing activity by conditioning visually evoked responses with selective cholinergic activation within V1. We found that activation of cholinergic innervation within V1 is indeed sufficient for cued interval-timing activity, in addition to it being necessary [6, 7]. These observations demonstrate the instructive role of basal forebrain and cholinergic innervation in educing visually cued timing to expected outcomes of behavioral relevance.

RESULTS

Behaviorally Conditioned Reward Timing in Mouse V1

Behaviorally conditioned reward-timing activity within V1 emerges as a consequence of pairing visual stimulation with delayed reward [6, 7]. Such conditioning results in a large proportion of V1 neurons with extended post-stimulus spike modulation (in the seconds range) that report accurately the delay, as experienced in the past, from the cue to its associated reward. This reward-timing activity is exhibited in three different response forms: those that express (1) a sustained increase in spiking until the expected reward time, (2) a sustained decrease in spiking until the expected reward time, and (3) a peak in spiking at the expected time of reward. As reward-timing activity has thus far been reported only in rats, we first sought here to evidence its presence in mice to demonstrate its generality to another species and establish mouse V1 as a model system for its mechanistic investigation.

We implanted adult C57/BL6 mice with multi-electrode drives to record extracellular single-unit activity in a cued, delayed-reward task. Behavioral and visually evoked responses to full-field retinal flash (100 ms) presented to the left or the right eye were conditioned by delivery of delayed water reward (Experimental Procedures; Figure S1A). Qualitatively, conditioned cues appeared to evoke V1 activity correlated with the expected reward times, as behaviorally experienced. Each of three previously reported reward-timing response forms were observed (sustained increase, sustained decrease, peak; Figure 1A, left, middle, right, respectively). We algorithmically characterized and sorted evoked responses into these three classes (Experimental Procedures; Figure S2), resulting in 64% (131 of 206) of evoked responses being so identified. According to the classified response form, a moment of post-stimulus time was then ascribed as the neural report of reward time (NRT, Experimental Procedures; Figure S3), which we interpret as the temporal expectancy of reward conveyed by the neural response.

If NRTs relate to the time of expected reward following visual stimulation as experienced in the past by the animal, then the central tendency of NRTs observed should accord with the central tendency of behaviorally experienced reward times (BRTs). Indeed, we found the median of the NRT distribution, observed per animal, to be indistinguishable (Figure 1B) from the median of the BRT distribution (mouse #, median NRT versus BRT, Wilcoxon rank-sum test p value: mouse #1, 1.15 versus 1.22 s, $p = 0.17$; mouse #2, 2.14 versus 2.16 s, $p = 0.44$; mouse #3, 1.90 versus 2.20 s, $p = 0.29$). In contrast, NRT distributions do not concord with the overall envelop of licking (Figure S1B). Together, these observations confirm and extend our previous reports of reward-timing activity from rat [6, 7] to mouse V1.

Selective Activation of BF Input within V1 Conditions "Reward" Timing

Having established the ability of mouse V1 to express reward-timing activity, we next tested the hypothesis [8, 31, 32] that the neural acquisition of visually cued reward timing is instructed by the activation of basal forebrain (BF) innervation of V1. We targeted BF nuclei known to innervate V1 directly in rodents [10, 11, 13, 14], namely, the diagonal band of Broca (DB, Figures S4B,

S4D, and S4E) and nucleus basalis/substantia innominata (nB/SI, Figures S4C, S4D, and S4E), for viral-mediated expression of channelrhodopsin (ChR2, Figures 2A and 2B; Experimental Procedures) to gain experimental control of the BF→V1 input. We found that in BF-infected animals receiving injection of a retrograde tracer in V1 (Experimental Procedures; Figure S4D), DB- and nB/SI-related structures were the only V1-projecting nuclei in the infected area (Figure S4E). Since in all identifiable V1-projecting nuclei the infection appeared to be restricted to BF (Figures S4E and S4F), we reasoned that BF→V1 input manipulation could be specifically achieved by adequate laser-light delivery [33, 34] through optical fibers implanted within V1 (Figures 2A and 2B; Experimental Procedures). Infected animals were then subjected to an optogenetic conditioning protocol (Figure 2C) designed to mimic the temporal relationship between visual stimulation and reinforcement signaling within V1, as presumptively experienced by their behaviorally conditioned counterparts.

Whether this manipulation leads to the neural expression of the interval between the cue and BF→V1 activation was assessed by analyzing conditioned cue-evoked responses (Experimental Procedures) in two cohorts of animals, one with a 1-s (Opto-1 s, n = 5) and the other with a 2-s (Opto-2 s, n = 7) delay to ChR2 activation. Optogenetic conditioning appeared, qualitatively, to result in neuronal responses that exhibited each of the three identified response forms observed in V1 following behavioral conditioning, with post-stimulus spike modulation corresponding to the delay between cue and ChR2-activation (Figure 3A, top row = Opto-1 s; bottom row = Opto-2 s; left to right columns: sustained increase, sustained decrease, and peak response). By subjecting the optogenetic data to the same response-classification and NRT-scoring algorithms used for analysis of behaviorally conditioned data, we found 35.7% (122 out of 342, Opto-1 s) and 44% (146 out of 332, Opto-2 s) of neural responses, respectively, to exhibit cue-evoked timing activity. The central tendency of NRTs for each experimental cohort (Figure 3B) accords with the corresponding optogenetically conditioned interval (median value = 1.16 s for Opto-1 s; 1.73 s for Opto-2 s). As observed following behavioral conditioning, distinctively entrained intervals in the two cohorts resulted in significantly different NRT medians (Figure 3C; $p < 10^{-7}$, Wilcoxon rank-sum test). This cue-evoked interval-timing activity is a consequence of selective activation of basal forebrain input since optogenetic conditioning and recordings from a control cohort (with GFP-only expression in BF→V1 projections, n = 3) resulted in, in the preponderance of cases, responses relating only to the presentations of the visual stimulus (see examples in Figure S5; only seven of 128, or 5.4% of responses, were identified by the same response-form classification scheme). Since basal forebrain is known to project widely across the cortical mantle [10, 14, 28], we further tested whether the optogenetic effects are specific to manipulations of BF→V1 inputs. In a separate cohort (n = 6) of animals receiving AAV-mediated ChR2 expression in BF, we paired visual stimulation with delayed (2 s) optogenetic activation of BF innervation of somatosensory cortex (S1, Figures 2D and 2E). Our analysis identified only 26/380 (6.8%) recorded neural responses in V1 with potential cued interval-timing features, a fraction expected by chance alone. In contrast to the activation of BF→V1 input, in which a large fraction of neural responses exhibited acutely modulated changes in spike rates (Figure S6), V1 neurons did not respond to optogenetic activation of BF→S1 input. This observation provides functional support to anatomical reports of topographically segregated corticopetal projections from BF [10, 11, 24, 35]. Together, these data show that delayed activation of basal forebrain input within V1 following visual stimulation is sufficient to engender neural representation of the conditioning interval in V1.

Cued Interval-Timing Activity Is Bidirectionally Modifiable

We have previously shown that behaviorally conditioned neural reports of time appropriately update to changes in the temporal relationships between cues and associated reward delays so as to conform with recent experience [6]. Therefore, we next investigated whether optogenetically conditioned V1 responses can similarly adapt to reflect a subsequent increase or decrease in the conditioning interval. To examine this, a subset of Opto-1 s (n = 3) and Opto-2 s (n = 4) animals were further conditioned to novel intervals of 2 s and 1 s, respectively, forming the Opto-1to2s and Opto-2to1s cohorts (Figures 4A and 4B). The new conditioning contingencies elicit all three response forms reported previously (Figure 4C). We found that the median of the NRT distribution from the Opto-2to1s cohort (Figure 4D) accords with the new conditioning interval (median = 1.01 s). In comparison to the median observed following initial conditioning to 2 s, decreasing the conditioning interval caused a corresponding and significant leftward shift in NRTs (solid versus dotted red curve in Figure 4F; $p < 10^{-7}$, Wilcoxon rank-sum test). Similarly, in the Opto-1to2s cohort (Figure 4E), the median of the NRT distribution accords with the new target interval (median = 1.80 s). The neural data from this group exhibited a significant rightward shift in the median compared to the initial conditioning to 1 s (solid versus dotted blue curve in Figure 4G; $p < 10^{-7}$, Wilcoxon rank-sum test). The proximity of the medians of the NRT distributions to their respective conditioned intervals, along with the significant difference of NRT distributions between Opto-2to1s and Opto-1to2s cohorts ($p < 10^{-7}$, Kolmogorov-Smirnov test), indicate that V1 activity can be bidirectionally modified, as observed following behavioral conditioning, to report newly imposed temporal contingencies between cue and BF→V1 input activation. Selective activation of BF→V1 projections therefore is sufficient for both the de novo synthesis and the bidirectional modification of cued interval-timing activity.

Experience-Dependent Refinement of the NRT Distribution

Optogenetic conditioning to the new delays in the second contingency (Opto-1to2s and Opto-1to2s cohorts) appeared to decrease the error of encoding the target time in comparison to that obtained under the first contingency (Opto-1 s and Opto-2 s cohorts, Figure S7). To quantify the error in reporting the target time, the absolute difference between individual NRTs and their respective target time was scored (difference from target, D_T). The difference between the error in reporting the target in the first versus second contingency was then assessed by comparing the cumulative distributions of D_T scores (Figure 5A), resulting in a significant leftward shift for the second

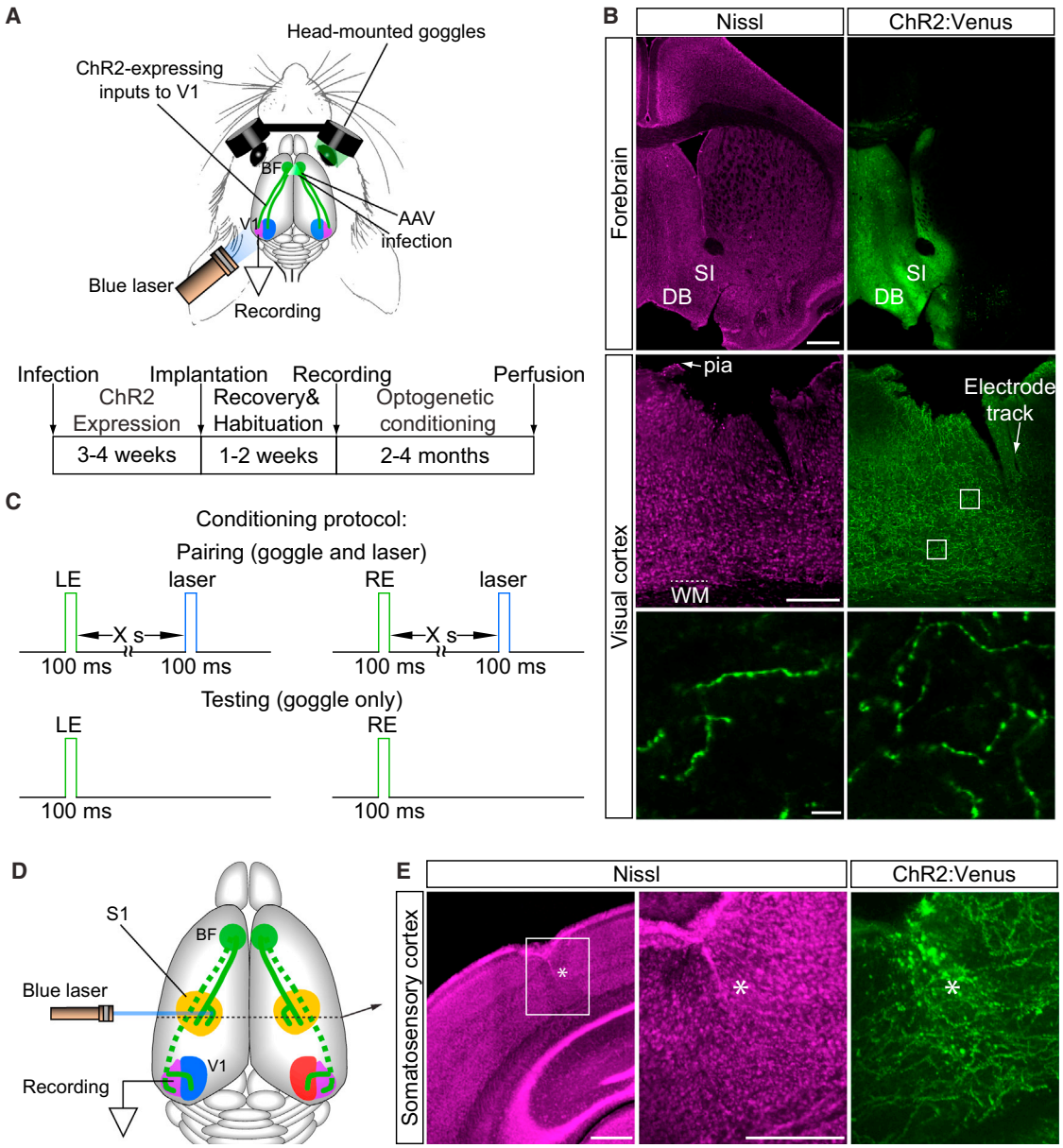

Figure 2. Selective Activation of BF Inputs

(A) Experimental design. BF nuclei were infected with recombinant AAV2/8 vectors carrying either a ChR2:Venus (experimental groups) or GFP-only (control groups) expression cassette. Multi-channel recording arrays and light guides for the activation of ChR2 were implanted in V1. Head-mounted goggles were used to present visual cues while recording from freely behaving animals. The timeline of the experimental procedure is shown below.

(B) Histology of ChR2:Venus expression. Confocal images taken from sections of an AAV2/8-ChR2:Venus infected animal. Top panel: a forebrain section with ChR2:Venus expression in targeted BF nuclei. Middle panel: a representative V1 section containing ChR2:Venus positive axons. Anatomical structures that accord with the Franklin and Paxinos atlas [52] were verified with Nissl staining (top and middle left). Arrow in the middle right panel indicates the track corresponding to an implanted electrode. Tissue damage due to implant removal is seen in the superficial layers. Bottom panel: higher-magnification views of boxed areas in V1 (from middle right) highlighting morphological details of ChR2:Venus-expressing axons. DB, the diagonal band of Broca; SI, substantia innominata; WM, white matter. Scale bar, 0.5 mm (top panel), 0.2 mm (middle panel), and 10 μm (bottom panel).

(C) Optogenetic conditioning protocol. Fixed-interval delays of BF→V1 input-activation (laser) following either the left (LE)- or right-eye (RE) stimulation (pairing trials) were designed to induce timing activity in V1. The effects of optogenetic conditioning on cue-evoked responses were assessed in interleaved trials with goggle-only stimulation (testing trials). The delay interval (X s) is 1 or 2 s, depending on the cohort (see Results).

(D) Experimental design for BF→S1 control animals. Following BF infection of AAV2/8-ChR2:Venus, an optical fiber light guide was implanted in primary somatosensory cortex (S1) for ChR2 activation. Recordings were made from multi-channel recording array implanted in V1 while the animal was optogenetically conditioned as indicate in (C). x = 2 s for the control animals.

(E) Histological confirmation of optical fiber implant in S1 in control cohort. An optical fiber track (in asterisk) in S1 was confirmed with Nissl staining (left and middle panel). ChR2-expressing axons can be seen in S1 (right panel). Scale bars, 400 μm.

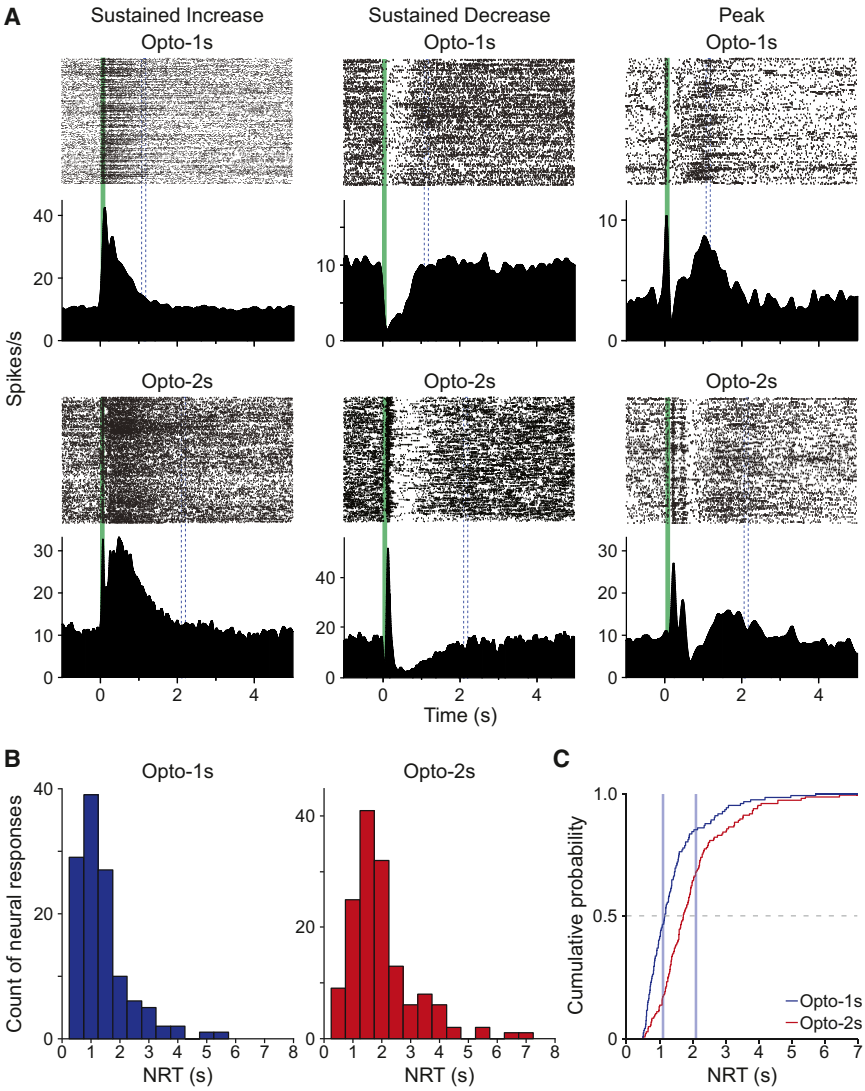

Figure 3. Cue-Evoked Neural Activity in V1 Reports Optogenetically Conditioned Intervals

(A) Cue-evoked responses following optogenetic conditioning. Examples of sustained increase (left), sustained decrease (middle), and peak (right) response forms that accord with the conditioned laser-time (dashed bars in blue) recorded from the Opto-1 s (top row) and Opto-2 s (bottom row) cohort. Cue presentations are shown as vertical bars in green.

(B) Histograms of NRT distributions. Left: data from the Opto-1 s cohort (n = 122). Right: data from the Opto-2 s cohort (n = 146).

(C) Cumulative distributions of population NRT. The time of laser presentation from stimulus onset is indicated by the vertical cyan bar (1.1–1.2 s for Opto-1 s and 2.1–2.2 s for Opto-2 s cohort, respectively). $p = 2 \times 10^{-7}$, Kolmogorov-Smirnov test.

contingency (p = 0.0081, Kolmogorov-Smirnov test). Best-fit gamma distributions for each of the cohorts that comprise the first and second contingencies (Figure S7) suggest that the precision of NRT distributions is increased under the second contingency (despite similar medians between cohorts encoding the same conditioning interval). To quantify the difference in precision, the absolute difference between individual NRTs and their respective cohorts' median was scored (difference from median, D_M). The difference between the precision observed in the first versus second contingency was then assessed by comparing the cumulative distributions of D_M scores (Figure 5B), resulting in a significant leftward shift for the second contingency (p = 0.0017, Kolmogorov-Smirnov test). Collectively, these comparisons indicate a refinement in the reporting of target time on account of training history.

NRT Distributions Exhibit a Scale Invariance to the Encoded Interval

The error exhibited by human and animal subjects in interval estimation scales proportionally to the duration of time examined, a phenomenon termed the "scalar timing property" [29, 30]. There have been numerous experimental reports in psychophysical and behavioral studies of the scalar timing property [29, 30], as well as recent experimental evidence of a neural correlate in higher-order cortex [36]. If reward-timing activity observed within V1 were involved in timing behaviors that abide by the scalar property, it should similarly express a scale invariance to the interval encoded. To examine this, the NRT distribution observed following behavioral conditioning using the 7-lick requirement (Behav-7licks, solid red in Figure 6A; data taken from mouse #1 in Figure 1B) was compared to that using the 10-lick requirement (Behav-10licks, solid blue in Figure 6A; data combined from mouse #2 and #3 in Figure 1B) by a multiplicative transformation. After scaling the Behav-7licks distribution by the ratio of the medians between the two distributions, the "scaled-up" distribution (Behav-7licks scaled, dotted red in Figure 6A) is indistinguishable to the Behav-10licks distribution (dotted red versus solid blue, Figure 6A; p = 0.66, Kolmogorov-Smirnov test). Therefore, behaviorally conditioned NRT distributions exhibit a scale invariance to the encoded interval, analogous to the temporal scalar property commonly observed behaviorally.

Since optogenetically conditioned responses are demonstrated to mimic reward-timing activity, we also assessed whether they exhibit this scale invariance. By multiplying the NRT distribution obtained from the Opto-1 s cohort by the ratio of the medians between the Opto-1 s and Opto-2 s cohorts, we found that the scaled-up data are superimposable with the Opto-2 s NRT distribution (dotted blue versus solid red, Figure 6B; p = 0.82, Kolmogorov-Smirnov test). This scale invariance in NRT distributions also holds true when similarly

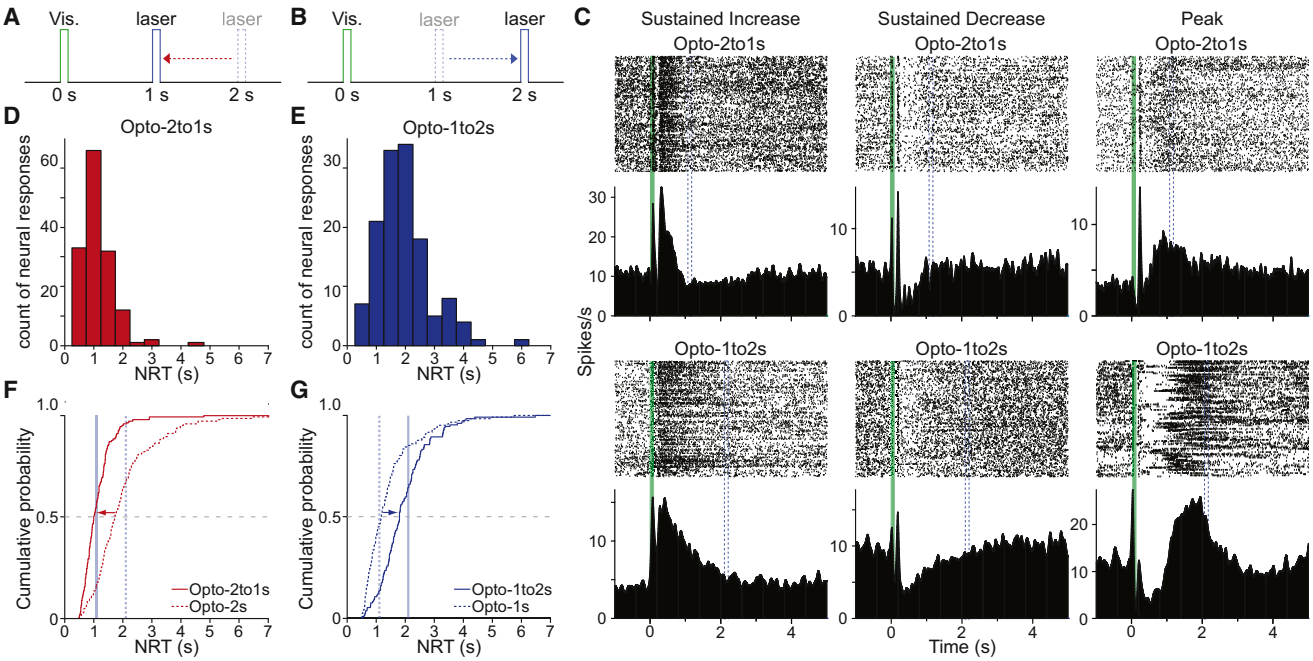

Figure 4. Bidirectional Modification of Neural Reports of Time

(A and B) Conditioning protocols for Opto-2to1s and Opto1to2s cohorts.

(C) Examples of sustained increase (left), sustained decrease (middle), and peak (right) response corresponding to the Opto-2to1s (top row) and Opto-1to2s (bottom row) cohort.

(D and E) Histograms of NRT from the Opto-2to1s (n = 147) and Opto-1to2s (n = 132) groups.

(F) Leftward shift of NRT distribution. Cumulative distribution of NRTs entrained to initial (Opto-2 s, dotted red curve) versus new (Opto-2to1s, solid red curve) target time ($p < 10^{-7}$, Kolmogorov-Smirnov test).

(G) Rightward shift of NRT distribution. Cumulative distribution of NRTs entrained to initial (Opto-1 s, dotted blue curve) versus new (Opto-1to2s, solid blue line) target time ($p < 10^{-7}$, Kolmogorov-Smirnov test). Vertical cyan bars in solid in (F) and (G) indicate the new target time from stimulus onset, while vertical cyan bars in dash indicate the initial target time from stimulus onset.

comparing data obtained from Opto-2to1s and Opto-1to2s cohorts (Figure 6C, dotted red versus solid blue; p = 0.67, Kolmogorov-Smirnov test), despite the decrease in the error of reporting the new target intervals. This multiplicative scaling resulted in a better fit to the observed data than an additive shift, an effect that also held for the behaviorally conditioned distributions (Table S1). Finally, when comparisons are made between optogenetically and behaviorally conditioned NRTs, scaled optogenetic data are indistinguishable from behavioral NRT distributions (Figures 6D and 6E; p = 0.63, Opto-1 s scaled versus Behav-7licks; p = 0.26, Opto-1 s scaled versus Behav-10licks; p = 0.81, Opto-2 s scaled versus Behav-7licks; p = 0.43, Opto-2 s scaled versus Behav-10licks; Kolmogorov-Smirnov test). Therefore, not only do optogenetically conditioned NRTs exhibit a scale invariance, but they also express a distribution that is similarly shaped to that generated following behavioral conditioning.

Selective Activation of Cholinergic Innervation within V1 Conditions Cued Interval-Timing Activity

Given that we have previously shown that lesioning cholinergic basal forebrain innervation within V1 impairs the learning of reward timing [6, 7], might optogenetically commandeering cholinergic innervation of V1 be sufficient to educe cued interval-timing activity? To test this, we employed a transgenic mouse line that expresses ChR2 under cholinergic-specific ChAT promoter control [37] to enable experimental manipulation of cholinergic innervation of V1. These animals (ChAT-ChR2) were then subjected to the same optogenetic conditioning protocol as before (Figure 2C), wherein visual stimulation is optogenetically conditioned to either a 1-s (ChAT-ChR2 1 s, n = 3) or a 2-s delay (ChAT-ChR2 2 s, n = 4). Optogenetic conditioning appeared qualitatively to result in neuronal responses that exhibited each of the three identified response forms (Figure 7A) observed in V1 following either behavioral or BF→V1 conditioning. Further analysis revealed that 35.8% (78 out of 218) of neural responses exhibited cued interval-timing activity in the ChAT-ChR2 1 s cohort, while 23.8% (93 out of 390) of neural responses were identified in the ChAT-ChR2 2 s cohort. NRT distributions in these two cohorts (Figure 7B) of ChAT-ChR2 mice are significantly different (median = 1.08 s for ChAT-ChR2 1 s, 1.65 s for ChAT-ChR2 2 s; p = 0.00002, Wilcoxon rank-sum test). Optogenetic conditioning of cholinergic input resulted in NRT distributions that were indistinguishable, however, to their respective BF→V1 (i.e., BF-ChR2 in Figure 7C) conditioned counterparts (Figure 7C; ChAT-ChR2 versus BF-ChR2: p = 0.72 for 1 s, 0.37 for 2 s, Wilcoxon rank-sum test). In a control cohort of ChAT-ChR2 animals (n = 4) receiving only visual stimulation, we did not observe cued interval-timing activity (only 11 of 194, or 5.7% of responses were identified by the response-form

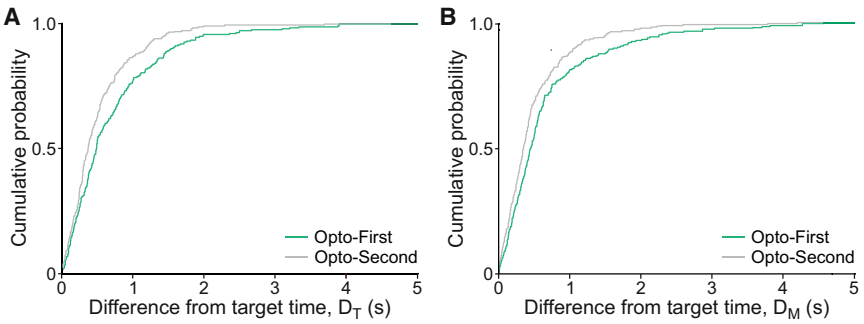

Figure 5. Experience-Dependent Refinement of Neural Reports of Conditioned Time

(A) A comparison of the error in reporting the target time observed under the first versus the second conditioning contingency. The absolute difference between individual NRTs and their corresponding target time (difference from target time, D_T) is plotted for the first (Opto-First: green, from Opto-1 s and Opto-2 s cohorts) and the second contingency (Opto-Second: gray, from Opto-2to1s and Opto-1to2s cohorts) as cumulative distributions.

(B) A comparison of the precision observed under the first versus the second contingency. The absolute difference between individual NRTs and their respective median (difference from median, D_M) are plotted as cumulative distributions for the first versus second contingencies.

classification scheme). Therefore, cholinergic activation within V1 is sufficient to encode visually cued timing activity to the conditioned intervals.

DISCUSSION

How brains learn and express the temporal interval between cues and expected outcomes is fundamental to the formation of adaptive behaviors, yet its physiological embodiment and mechanistic underpinnings are not well understood. Reward-timing activity within V1 exemplifies the neural expression of learned temporal intervals of behavioral import associated with external cues. Its observation proffers the questions of where, how, and why this activity is generated. To facilitate a mechanistic investigation, we began by first establishing the presence of reward-timing activity in mouse visual cortex, corroborating our prior findings in rat [6, 7] and affording a means of bringing putative reinforcement signals under experimental control using transgenic mice. Behavioral conditioning of visual cues with delayed reward induces in V1 post-stimulus activity—exhibiting three response forms—that correlates with the time of expected reward. We next demonstrated that selective activation of basal forebrain input within visual cortex is sufficient to condition stimulus-evoked neural responses that mimic behaviorally conditioned reward-timing activity. Optogenetically conditioned V1 activity not only accords with conditioned intervals, but also is bidirectionally modifiable, updating to changes in cue-"reward" delay and exhibits experience-dependent refinement. Further, similar to behaviorally conditioned reward-timing activity, we found that optogenetically conditioned "reward"-timing activity is scale invariant to the interval encoded, a presumptive neuronal hallmark of the temporal scalar property [29, 30]. Finally, optogenetically commandeering cholinergic innervation within V1 is sufficient in and of itself to instill cued interval-timing activity in vivo. Collectively, these observations advance an understanding of the neural mechanisms and properties of interval timing elicited by cues that are predictive of upcoming, behaviorally relevant outcomes.

So where and how is this cued interval-timing activity generated? Persistent or ramping activity recorded in higher-order brain regions (e.g., the frontal [38] and parietal [39] areas) bears resemblance to reward-timing activity observed in V1 and has also been interpreted as relating behaviorally relevant timing information [1, 3, 38, 39]. Therefore, it may reasonably be presumed that reward timing could be present in V1 simply as a consequence of V1 being privy, via feedback connections, to learning induced changes elicited elsewhere. Alternatively, rather than simply being the recipient of "top-down" information, V1 may itself actively transform input regarding visual cues into temporally extensive responses predictive of upcoming reward. Here, we demonstrate that V1 is likely the site of learning the observed reward-timing activity by selectively activating corticopetal innervation in V1 following visual stimulation, thereby engendering visually cued interval timing that mimics reward-timing activity. Therefore, as we have previously shown that lesioning of BF input impairs the ability of V1 to bidirectionally modify reward-timing activity [6], our new results indicate that BF input is not only necessary but also sufficient for the bidirectional modification of cued interval timing. More fundamentally, selective activation of BF or cholinergic input is sufficient for the de novo synthesis of cued interval-timing activity. That V1 is the site of learning this activity is consonant with BF- and cholinergic-dependent cortical plasticity reported in primary sensory areas [6, 23–25, 40–42]. As it has recently been shown that both appetitive and aversive conditioning activates specific types of cortical neurons in primary sensory areas through cholinergic pathways [43–45], further investigation of the contribution of these neurons will provide a deeper understanding of the neural circuit involved in learning cued interval-timing activity.

There is mounting evidence indicating behavioral state- and context-dependent modulation [35, 36, 46–48] of stimulus-evoked V1 responses. As BF projections are implicated in these processes [24, 35, 46, 49], a reasonable assumption is that they contribute to reward-timing activity through modulating cortical states during task performance. However, as optogenetically conditioned cued interval-timing activity is entrained in the absence of a behavioral task, an accounting of observed interval-timing activity based on behavioral state- and/or context-dependent modulation seems unlikely. In addition to the effects of gain modulation of visual responses by electrical stimulation of BF input [46] or optogenetic activation of cholinergic innervations in V1 [35], the results here indicate another role for BF and cholinergic projections in conveying the outcome

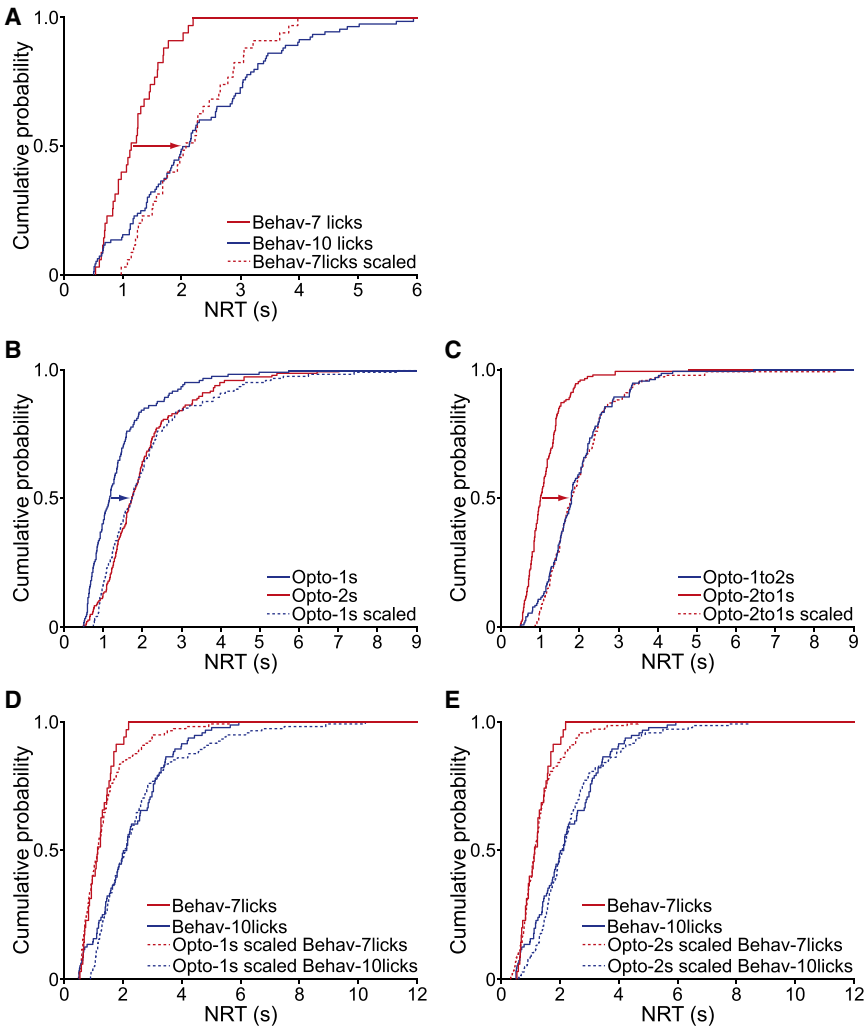

Figure 6. NRT Distributions Exhibit Scale Invariance and Are Similarly Shaped within and between Behaviorally and Optogenetically Conditioned Cohorts

(A) NRT distributions observed following behavioral conditioning using the 7- (Behav-7licks, solid red) or 10-lick (Behav-10licks, solid blue) requirement are compared by scaling-up the Behav-7licks distribution (Behav-7licks scaled, dotted red).

(B) Scaled comparison between optogenetically conditioned NRT distributions (Opto-1 s, solid blue; Opto-2 s, solid red; Opto-1 s scaled, dotted red).

(C) Scaled comparison between cohorts conditioned to new target time. Opto-2to1s, solid red; Opto-1to2s, solid blue; Opto-2to1s scaled, dotted red.

(D and E) Superposition of scaled optogenetic data and original behavioral NRTs. Data labels as indicated (see details in Results).

associated with predictive visual cues, thereby instructing learning of the cue-reward interval.

To what end is this activity generated? We propose that cued interval timing in V1 signifies an internal model of the world is constructed that conveys temporal expectations of future, behaviorally relevant events. In addition, two novel properties of cued interval timing in V1 revealed in this study—its experience-dependent refinement and scalar invariance—suggest that it is also possible that V1 participates in interval timing. Indeed, in contemporaneous work, we demonstrate that cued interval-timing activity within V1 may inform the timing of visually cued actions by the animal in its effort to maximize reward [50]. These observations lend behavioral relevance to investigating the mechanism by which cued interval-timing activity comes about in V1.

In summary, V1 provides a model system in which the neural genesis of temporal intervals of behavioral import may be investigated. We demonstrate that basal forebrain or cholinergic innervation of V1 is sufficient for conditioning cued interval-timing activity, and that V1 itself is a substrate for learning and expressing cue-reward intervals. These findings corroborate a formal framework [8, 31, 32] for learning reward timing, a domain commonly considered the province of "higher" cortical regions, and advance a mechanistic understanding of reinforcement [5] and associative learning.

EXPERIMENTAL PROCEDURES

Animals

All animal procedures were conducted in accordance with the U.S. NIH Guide for the Care and Use of Laboratory Animals and were approved by The Johns Hopkins University Institutional Animal Care and Use Committee. Adult male C57Bl/6 mice (≥P30; Jackson Laboratory) were used for all behavioral and optogenetic experiments. ChAT-ChR2 mice for optogenetic experiments were derived from Dr. Guoping Feng at the Massachusetts Institute of Technology [37]. Animals were housed in a satellite facility with 12-hr-dark/12-hr-light cycle control, in which lights were provided from 07:00 to 19:00.

Surgical Procedures

Animal surgeries were performed in accordance to the guidelines from The Johns Hopkins University Institutional Animal Care and Use Committee. All surgeries were conducted under sterile conditions with ketamine/xylazine anesthesia (50/10 mg kg^{-1}, intraperitoneal). For animals used in behavioral conditioning experiments, custom-made 16-channel microdrives for single-unit activity recordings were implanted in the binocular segment of V1 [51]. In optogenetic conditioning experiments, virally infected animals (see below) and ChAT-ChR2 transgenic mice were implanted with multichannel recording arrays coupled to optical fibers (200 μm in core diameter, NA = 0.22, A.R.T. Photonics, Germany) for blue laser-light delivery in V1. The effects of BF→V1input-activation on cued interval timing were compared to a control cohort of infected animals presented with the same visual stimuli but conditioned by optogenetic activation of BF input within primary somatosensory cortex (S1, see below). Implanting and recording sites were confirmed histologically.

To achieve channelrhodopsin (ChR2) expression, adeno-associated virus (AAV2, serotype 8) carrying the ChR2:Venus cassette (ChR2:Venus is from Addgene plasmid 15753, pCAGG-ChR2:Venus; DNA cloned by Rachael Neve at the MIT Viral Vector Core into Virovek's plasmid backbone pFB-AAV-CMV-SV40 and packaged by Virovek, titer ~1e12 viral particles/ml)

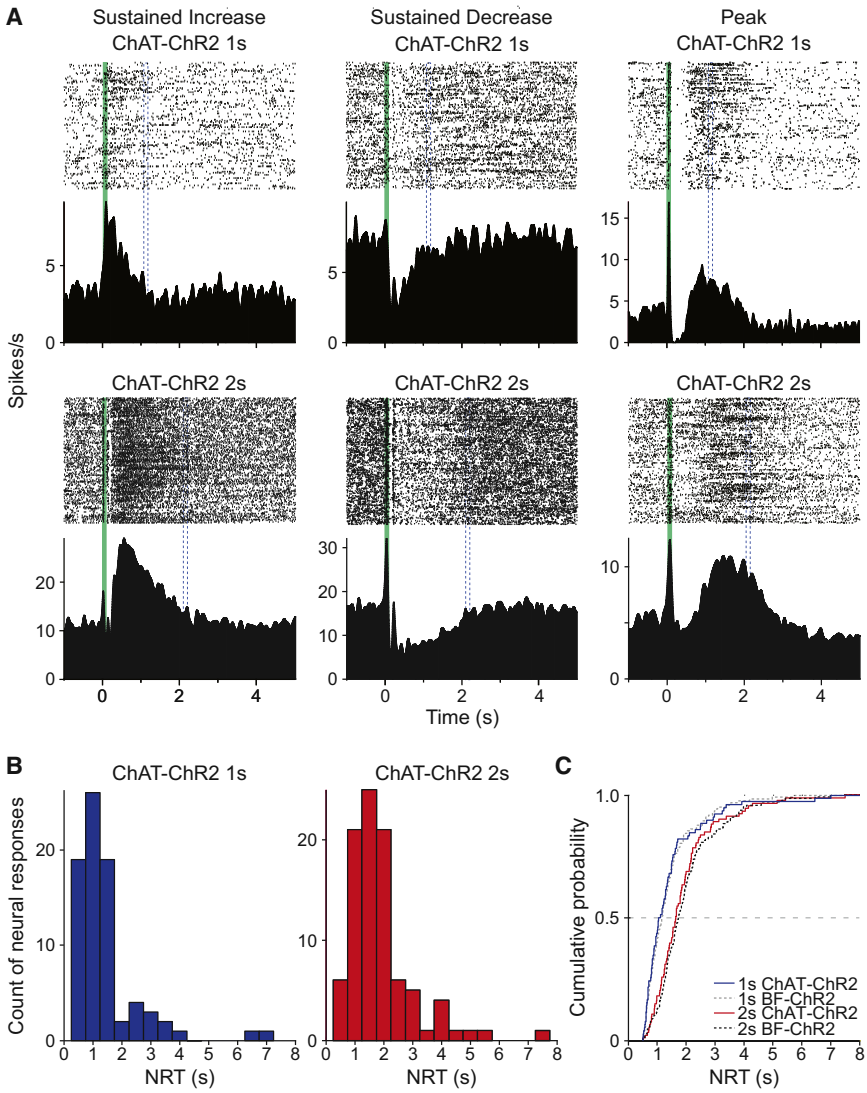

Figure 7. Optogenetic Activation of Cholinergic Innervation within V1 Is Sufficient to Engender Cued Interval-Timing Activity

(A) Examples of response forms recorded from V1 of conditioned ChAT-ChR2 mice. Sustained increase (left), sustained decrease (middle), and peak (right) responses were found in animals conditioned to either a 1-s (ChAT-ChR2 1 s, top row) or a 2-s (ChAT-ChR2 2 s, bottom row) delay, like that shown in Figure 2C. Green vertical bars, visual stimulation. Dashed blue bars, time of laser stimulation.

(B) Histograms of NRT distributions from the two conditioned cohorts.

(C) Comparison of cumulative NRT distributions within and between conditioned ChAT-ChR2 and BF-ChR2 cohorts. NRT distributions are significantly different between ChAT-ChR2 cohorts conditioned to 1-s (solid blue) and 2-s (solid red) delays ($p = 0.0003$, Kolmogorov-Smirnov test). Further, comparisons of cumulative NRTs between ChAT-ChR2 and BF-ChR2 cohorts (dashed gray = 1 s and black = 2 s) conditioned to the same delay demonstrate that they are indistinguishable (1 s: $p = 0.98$, Kolmogorov-Smirnov test; 2 s: $p = 0.77$, Kolmogorov-Smirnov test). BF-ChR2 data are the same as in Figure 3C.

was injected into basal forebrain (BF) nuclei using a Nanoject II (Drummond Scientific). The stereotaxic coordinates (from bregma) for targeted areas [52] are as follows: (1) nucleus basalis/substantia innominata (NB/SI), 0.55 mm posterior; 1.75 mm lateral; 4.2 and 3.8 mm ventral; (2) ventral limb of the diagonal band, 0.75 mm anterior; 0.18 mm lateral; 4.55 and 4.05 mm ventral; (3) horizontal limb of the diagonal band, 0.5 mm anterior; 0.9 mm lateral; 5.2 and 5 mm ventral. At each penetration depth, 276 nl of viral solution was injected. In a control group of ChR2-infected animals, visual stimulation was conditioned with delayed (2 s) activation of BF input in S1 by optical fibers implanted in stereotaxic coordinates corresponding to S1 (from bregma: 1.94 mm posterior; 3.2 mm lateral; 0.3 mm ventral). Another group of animals were injected with AAV2/8-CMV-GFP and used as controls for optogenetic experiments. ChR2:Venus and GFP expression in BF, BF→V1, and BF→S1 projections were histologically verified.

To verify the infection specificity and efficiency of V1-projecting neurons in BF, a cohort of animals receiving AAV (n = 3 with ChR2:Venus and n = 1 with GFP) infection using the same protocol were injected with the retrograde tracer fluorogold (FG, Sigma-Aldrich; 2.0% in PBS, 200 nl) in V1 at sites corresponding to the location of electrode implants (Figure S4D). Serial sections containing BF nuclei (Figures S4D and S4E) were selected for calculating the percentage of retrogradely labeled V1-projecting neurons with ChR2:Venus or GFP expression. We found that 54% ± 5% of FG-labeled neurons in BF (50% ± 8% in NB/SI, 61% ± 6% in VDB and HDB) were infected by the protocol. Conversely, we were unable to detect AAV-mediated protein expression in areas exhibiting strong FG labeling outside of BF (Figure S4F).

Electrophysiology

Data from extracellularly recorded neural signals were digitally sampled at 33 kHz and stored by the Digital Lynx (Neuralynx) system. Single-unit activity from band-pass filtered (1–10 kHz) signals was isolated using commercial software (OfflineSorter, Plexon). Experimental events during behavioral (visual stimulations and reward deliveries) and optogenetic (visual stimulations and laser illuminations) conditioning were output from a custom-assembled module and controlled by user-defined MATLAB (MathWorks) programs. Time stamps for these events were collected by Digital Lynx, and peri-stimulus time histograms of spiking activity were compiled and displayed using the NeuroExplorer (Plexon) software. Data analysis was accomplished by programs written in MATLAB.

Behavioral Conditioning

Implanted animals were allowed 5–7 days to recover post-surgery before being subjected to water restriction in their home cages. A schedule for water restriction was carefully designed and closely monitored so that the weights of deprived animals were maintained at >90% of their initial body weights. Behavioral conditioning for the reward-timing task was performed similarly to the protocol previously described [7]. In brief, water-deprived animals received full-retinal illuminations (100 ms) to either the left- or right-eye through a pair of head-mounted goggles as the conditioning cues when accessing the nose poke in the training apparatus. Solenoid-controlled delivery of water was achieved by licking the reward port for the designated number of times. The required number of licks for reward administration is the same for both left- and right-eye stimulation in each animal. Equal numbers of rewarded and unrewarded (catch) trials were pseudo-randomly presented to the animal. While mice initially exhibited excessive licking behavior in interleaved unrewarded trials, they learned to reduce the number of licks emitted following the required number to receive reward (Figure S1A). We used only data recorded from

unrewarded trials for response-form classification and NRT scoring (see Data Analysis).

Optogenetic Conditioning

The timeline for optogenetic conditioning experiments is schematized in Figure 2A. Animals were allowed food and water access ad libitum in their home cages post-infection. We found that a minimal of 3 weeks post-infection was required for detectable ChR2:Venus expression in V1. ChR2 was activated by blue laser (473 nm, 500–650 μW, 100 ms) delivered through implanted optical fiber (350 ± 50 μm below pia). When optogenetically conditioned, animals were placed in the same training apparatus used for behavioral conditioning and allowed to explore freely. Comparable numbers of four different trial types (Figure 2C) were pseudo-randomly presented, and separated by randomized inter-trial intervals ranging between 5 and 7 s. To activate ChR2 expressed on BF→V1 input, brief (100 ms) illumination of blue laser light (473 nm) was delivered through locally implanted optical fiber in V1. Laser stimulation appeared to transiently modulate firing rates in ChR2-infected animals (Figure S6), but not in GFP-infected controls. Scored by visual inspection, approximately half (368/704) of neurons recorded from ChR2-infected animals displayed laser-modulated activity changes, indicating efficacious optogenetic control of BF→V1 input. To calculate optogenetically conditioned neural reports of time (see below), we scored data from the trials in which laser stimulation was withheld following visual stimulation (the goggle-only, "catch" trials). The same laser-stimulation protocol was used for the control cohort with S1 optical fiber implantation.

Data Analysis: Detection, Classification, and Determination of Neural Reports of Time

In order to identify, classify, and score cue-evoked timing activity, we first selected a subset of neural responses characteristic of the three previously described [7] reward-timing response-forms (n = 95 for sustained increase, 117 for sustained decrease, and 35 for peak responses; Figure S2A) to constitute a template for objective response form identification and classification. The post-stimulus (>500 ms following visual stimulation) activity of these 247 neural responses was subjected to principal component (PC) analysis. Projecting the template data in a space defined by the first four PCs (which accounted for >70% of the total variance, Figure S2B) resulted in clusters populated, predominantly, by responses that had been manually classified as sustained increase, sustained decrease, and peak responses (as illustrated by the projection pattern in the first three PCs, Figure S2C). In order to achieve objective data classification with a Bayesian decision method, we deduced a template corresponding to the individual clusters from the mean and covariance matrices by assuming within-cluster multivariate Gaussian distributions of data [53]. Overall, this template categorized 87.4% (216/247) of the selected data into classes that agreed with response forms as manually assigned (Figure S2D).

This template was subsequently used to detect and classify putative reward-timing responses from all of the data collected. Objective membership assignment of response form was achieved by determining the relative probabilities of a neural response being associated with the three individual clusters in the template. Setting a threshold of 75% relative probability from template clusters resulted in categorization that accorded well with subjective classification achieved through visual inspection while separating neural responses with putative timing features from those with no discernible cue-evoked activity or with only transient stimulus-evoked responses (as examples in Figure S5).

Following response-form classification, we determined the neural report of time (NRT) for each classified response. This was done by first determining the spontaneous activity level, characterized as a bounded range (defined by the upper and lower threshold in Figure S3A) that encompassed the pre-stimulus firing-rate fluctuations. The bounded range was set to capture 95% of the distribution of pre-stimulus firing rates in optogenetic experiments. As animals performed fewer trials during behavioral conditioning, this range was set to contain 85% of the distribution of pre-stimulus firing rates in behavioral experiments. This bounded range served to determine moments in time in which the post-stimulus activity was comparable to its pre-stimulus firing rate. In order to exclude from the analysis the contribution of spike modulation driven directly by the stimulus itself, we limited NRT analysis to data collected >500 ms from stimulus onset. For the sustained increase response form, the NRT algorithm identified the first post-stimulus moment in which the firing rate crossed below the upper threshold of pre-stimulus activity and remained so for at least 100 ms (Figure S3A1). Similarly, for the sustained decrease response form (Figure S3A2), we assessed the first post-stimulus moment in which the firing rate crossed above the lower threshold and remained so for at least 100 ms. For the peak response form, the NRT algorithm determined the first post-stimulus time window (continuous for ≥200 ms) during which firing rates were outside of the bounded range, and set the NRT as the moment of maximal deviation from spontaneous firing within this window (Figure S3A3). We tested the reliability of the results determined by this algorithm and found that NRTs are robust to changes in the Gaussian filtering of the neural responses (Figure S3B).

SUPPLEMENTAL INFORMATION

Supplemental Information includes seven figures and one table and can be found with this article online at http://dx.doi.org/10.1016/j.cub.2015.04.028.

AUTHOR CONTRIBUTIONS

The experiments were conceived and designed by M.G.H.S. and C.-H.L. C.-H.L. performed the experiments and collected and analyzed the data. H.D. and K.Z. contributed to data analysis and software programming. J.E.C. provided reagents for optogenetic experiments and assisted in anatomical and histological analyses. M.G.H.S. and C.-H.L. wrote the manuscript.

ACKNOWLEDGMENTS

This work was supported by NIH (R01MH084911 and R01MH093665) and a grant from the Brain Science Institute and the Science of Learning Institute at Johns Hopkins. We thank R. Gujarati, D. Reyes-Capo, D. Sundermann, M. Szaro, and H. Zhang for assisting in experimental setup and data collection and M. Bear, R. Cudmore, E. Hughes, D. Nguyen, and H. Shouval for discussions and comments on the manuscript. We also thank H. Zhang for assistance on histology and G. Feng for providing the ChAT-ChR2 mouse line.

Received: October 3, 2014
Revised: March 16, 2015
Accepted: April 14, 2015
Published: May 21, 2015

REFERENCES

1. Leon, M.I., and Shadlen, M.N. (2003). Representation of time by neurons in the posterior parietal cortex of the macaque. Neuron *38*, 317–327.
2. Mauk, M.D., Steinmetz, J.E., and Thompson, R.F. (1986). Classical conditioning using stimulation of the inferior olive as the unconditioned stimulus. Proc. Natl. Acad. Sci. USA *83*, 5349–5353.
3. Mita, A., Mushiake, H., Shima, K., Matsuzaka, Y., and Tanji, J. (2009). Interval time coding by neurons in the presupplementary and supplementary motor areas. Nat. Neurosci. *12*, 502–507.
4. Schultz, W., Apicella, P., Scarnati, E., and Ljungberg, T. (1992). Neuronal activity in monkey ventral striatum related to the expectation of reward. J. Neurosci. *12*, 4595–4610.
5. Dayan, P., and Niv, Y. (2008). Reinforcement learning: the good, the bad and the ugly. Curr. Opin. Neurobiol. *18*, 185–196.
6. Chubykin, A.A., Roach, E.B., Bear, M.F., and Shuler, M.G. (2013). A cholinergic mechanism for reward timing within primary visual cortex. Neuron *77*, 723–735.
7. Shuler, M.G., and Bear, M.F. (2006). Reward timing in the primary visual cortex. Science *311*, 1606–1609.
8. Gavornik, J.P., Shuler, M.G., Loewenstein, Y., Bear, M.F., and Shouval, H.Z. (2009). Learning reward timing in cortex through reward dependent expression of synaptic plasticity. Proc. Natl. Acad. Sci. USA *106*, 6826–6831.
9. Sutton, R.S., and Barto, A.G. (1998). Reinforcement Learning. (MIT Press).

10. Bigl, V., Woolf, N.J., and Butcher, L.L. (1982). Cholinergic projections from the basal forebrain to frontal, parietal, temporal, occipital, and cingulate cortices: a combined fluorescent tracer and acetylcholinesterase analysis. Brain Res. Bull. *8*, 727–749.
11. Carey, R.G., and Rieck, R.W. (1987). Topographic projections to the visual cortex from the basal forebrain in the rat. Brain Res. *424*, 205–215.
12. Moreau, P.H., Cosquer, B., Jeltsch, H., Cassel, J.C., and Mathis, C. (2008). Neuroanatomical and behavioral effects of a novel version of the cholinergic immunotoxin mu p75-saporin in mice. Hippocampus *18*, 610–622.
13. Rieck, R., and Carey, R.G. (1984). Evidence for a laminar organization of basal forebrain afferents to the visual cortex. Brain Res. *297*, 374–380.
14. Rye, D.B., Wainer, B.H., Mesulam, M.M., Mufson, E.J., and Saper, C.B. (1984). Cortical projections arising from the basal forebrain: a study of cholinergic and noncholinergic components employing combined retrograde tracing and immunohistochemical localization of choline acetyltransferase. Neuroscience *13*, 627–643.
15. Masuda, R., Fukuda, M., Ono, T., and Endo, S. (1997). Neuronal responses at the sight of objects in monkey basal forebrain subregions during operant visual tasks. Neurobiol. Learn. Mem. *67*, 181–196.
16. Richardson, R.T., and DeLong, M.R. (1991). Electrophysiological studies of the functions of the nucleus basalis in primates. Adv. Exp. Med. Biol. *295*, 233–252.
17. Wilson, F.A., and Ma, Y.Y. (2004). Reinforcement-related neurons in the primate basal forebrain respond to the learned significance of task events rather than to the hedonic attributes of reward. Brain Res. Cogn. Brain Res. *19*, 74–81.
18. Robinson, B.W., and Mishkin, M. (1968). Alimentary responses to forebrain stimulation in monkeys. Exp. Brain Res. *4*, 330–366.
19. Fekete, M., Bohus, B., Van Wolfswinkel, L., Van Ree, J.M., and De Wied, D. (1982). Comparative effects of the ACTH 4-9 analogue (ORG 2766), ACTH 4-10 and [D-Phe7] ACTH 4-10 on medial septal self-stimulation behaviour in rats. Neuropharmacology *21*, 909–916.
20. Coyle, J.T., Price, D.L., and DeLong, M.R. (1983). Alzheimer's disease: a disorder of cortical cholinergic innervation. Science *219*, 1184–1190.
21. Dekker, A.J., Connor, D.J., and Thal, L.J. (1991). The role of cholinergic projections from the nucleus basalis in memory. Neurosci. Biobehav. Rev. *15*, 299–317.
22. Buzsaki, G., Bickford, R.G., Ponomareff, G., Thal, L.J., Mandel, R., and Gage, F.H. (1988). Nucleus basalis and thalamic control of neocortical activity in the freely moving rat. J. Neurosci. *8*, 4007–4026.
23. Froemke, R.C., Merzenich, M.M., and Schreiner, C.E. (2007). A synaptic memory trace for cortical receptive field plasticity. Nature *450*, 425–429.
24. Kang, J.I., and Vaucher, E. (2009). Cholinergic pairing with visual activation results in long-term enhancement of visual evoked potentials. PLoS ONE *4*, e5995.
25. Kilgard, M.P., and Merzenich, M.M. (1998). Cortical map reorganization enabled by nucleus basalis activity. Science *279*, 1714–1718.
26. Lin, S.C., and Nicolelis, M.A. (2008). Neuronal ensemble bursting in the basal forebrain encodes salience irrespective of valence. Neuron *59*, 138–149.
27. Manns, I.D., Alonso, A., and Jones, B.E. (2003). Rhythmically discharging basal forebrain units comprise cholinergic, GABAergic, and putative glutamatergic cells. J. Neurophysiol. *89*, 1057–1066.
28. Zaborszky, L., Pang, K., Somogyi, J., Nadasdy, Z., and Kallo, I. (1999). The basal forebrain corticopetal system revisited. Ann. N Y Acad. Sci. *877*, 339–367.
29. Gallistel, C.R., and Gibbon, J. (2000). Time, rate, and conditioning. Psychol. Rev. *107*, 289–344.
30. Gibbon, J., Malapani, C., Dale, C.L., and Gallistel, C. (1997). Toward a neurobiology of temporal cognition: advances and challenges. Curr. Opin. Neurobiol. *7*, 170–184.
31. Gavornik, J.P., and Shouval, H.Z. (2011). A network of spiking neurons that can represent interval timing: mean field analysis. J. Comput. Neurosci. *30*, 501–513.
32. Shouval, H.Z., and Gavornik, J.P. (2011). A single spiking neuron that can represent interval timing: analysis, plasticity and multi-stability. J. Comput. Neurosci. *30*, 489–499.
33. Aravanis, A.M., Wang, L.P., Zhang, F., Meltzer, L.A., Mogri, M.Z., Schneider, M.B., and Deisseroth, K. (2007). An optical neural interface: in vivo control of rodent motor cortex with integrated fiberoptic and optogenetic technology. J. Neural Eng. *4*, S143–S156.
34. Yizhar, O., Fenno, L.E., Davidson, T.J., Mogri, M., and Deisseroth, K. (2011). Optogenetics in neural systems. Neuron *71*, 9–34.
35. Pinto, L., Goard, M.J., Estandian, D., Xu, M., Kwan, A.C., Lee, S.H., Harrison, T.C., Feng, G., and Dan, Y. (2013). Fast modulation of visual perception by basal forebrain cholinergic neurons. Nat. Neurosci. *16*, 1857–1863.
36. Xu, M., Zhang, S.Y., Dan, Y., and Poo, M.M. (2014). Representation of interval timing by temporally scalable firing patterns in rat prefrontal cortex. Proc. Natl. Acad. Sci. USA *111*, 480–485.
37. Zhao, S., Ting, J.T., Atallah, H.E., Qiu, L., Tan, J., Gloss, B., Augustine, G.J., Deisseroth, K., Luo, M., Graybiel, A.M., and Feng, G. (2011). Cell type–specific channelrhodopsin-2 transgenic mice for optogenetic dissection of neural circuitry function. Nat. Methods *8*, 745–752.
38. Goldman-Rakic, P.S. (1995). Cellular basis of working memory. Neuron *14*, 477–485.
39. Janssen, P., and Shadlen, M.N. (2005). A representation of the hazard rate of elapsed time in macaque area LIP. Nat. Neurosci. *8*, 234–241.
40. Miasnikov, A.A., Chen, J.C., and Weinberger, N.M. (2008). Specific auditory memory induced by nucleus basalis stimulation depends on intrinsic acetylcholine. Neurobiol. Learn. Mem. *90*, 443–454.
41. Sachdev, R.N., Lu, S.M., Wiley, R.G., and Ebner, F.F. (1998). Role of the basal forebrain cholinergic projection in somatosensory cortical plasticity. J. Neurophysiol. *79*, 3216–3228.
42. Shulz, D.E., Ego-Stengel, V., and Ahissar, E. (2003). Acetylcholine-dependent potentiation of temporal frequency representation in the barrel cortex does not depend on response magnitude during conditioning. J. Physiol. Paris *97*, 431–439.
43. Alitto, H.J., and Dan, Y. (2012). Cell-type-specific modulation of neocortical activity by basal forebrain input. Front. Syst. Neurosci. *6*, 79.
44. Letzkus, J.J., Wolff, S.B., Meyer, E.M., Tovote, P., Courtin, J., Herry, C., and Lüthi, A. (2011). A disinhibitory microcircuit for associative fear learning in the auditory cortex. Nature *480*, 331–335.
45. Pi, H.J., Hangya, B., Kvitsiani, D., Sanders, J.I., Huang, Z.J., and Kepecs, A. (2013). Cortical interneurons that specialize in disinhibitory control. Nature *503*, 521–524.
46. Goard, M., and Dan, Y. (2009). Basal forebrain activation enhances cortical coding of natural scenes. Nat. Neurosci. *12*, 1444–1449.
47. Niell, C.M., and Stryker, M.P. (2010). Modulation of visual responses by behavioral state in mouse visual cortex. Neuron *65*, 472–479.
48. Szuts, T.A., Fadeyev, V., Kachiguine, S., Sher, A., Grivich, M.V., Agrochão, M., Hottowy, P., Dabrowski, W., Lubenov, E.V., Siapas, A.G., et al. (2011). A wireless multi-channel neural amplifier for freely moving animals. Nat. Neurosci. *14*, 263–269.
49. Herrero, J.L., Roberts, M.J., Delicato, L.S., Gieselmann, M.A., Dayan, P., and Thiele, A. (2008). Acetylcholine contributes through muscarinic receptors to attentional modulation in V1. Nature *454*, 1110–1114.
50. Namboodiri, V.M.K., Huertas, M.A., Monk, K.J., Shouval, H.Z., and Hussain Shuler, M.G. (2015). Visually cued action timing in the primary visual cortex. Neuron *86*, 319–330.
51. Liu, C.H., Heynen, A.J., Shuler, M.G., and Bear, M.F. (2008). Cannabinoid receptor blockade reveals parallel plasticity mechanisms in different layers of mouse visual cortex. Neuron *58*, 340–345.
52. Franklin, K., and Paxinos, G. (2008). The Mouse Brain in Stereotaxic Coordinates, Third Edition. (Elsevier).
53. Duda, R.E., Hart, P.E., and Stork, D.G. (2001). Pattern Classification, Second Edition. (Wiley).